ResearchGate

See discussions, stats, and author profiles for this publication at: https://www.researchgate.net/publication/7287054

Size, Charge, and Interactions with Giant Lipid Vesicles of Quantum Dots Coated with an Amphiphilic Macromolecule

ARTICLE *in* LANGMUIR · MARCH 2006

Impact Factor: 4.46 · DOI: 10.1021/la052704y · Source: PubMed

CITATIONS
93

READS
71

5 AUTHORS, INCLUDING:

Camilla Luccardini
Claude Bernard University Lyon 1
23 PUBLICATIONS **1,688** CITATIONS
SEE PROFILE

Christophe Tribet
Ecole Normale Supérieure de Paris
85 PUBLICATIONS **2,609** CITATIONS
SEE PROFILE

Valérie Marchi-Artzner
French National centre for scientific research…
47 PUBLICATIONS **1,548** CITATIONS
SEE PROFILE

Maxime Dahan
Institut Curie
163 PUBLICATIONS **6,508** CITATIONS
SEE PROFILE

Available from: Maxime Dahan
Retrieved on: 27 January 2016

Size, Charge, and Interactions with Giant Lipid Vesicles of Quantum Dots Coated with an Amphiphilic Macromolecule

C. Luccardini,[†] C. Tribet,*[,‡] F. Vial,[‡] V. Marchi-Artzner,[§] and M. Dahan*[,†]

Laboratoire Kastler Brossel, CNRS UMR8552, Ecole normale supérieure et Université Pierre et Marie Curie−Paris 6, 24 rue Lhomond 75005 Paris, France, Physico-chimie des Polymères et des Milieux Dispersés, CNRS UMR 7615 et Université Pierre et Marie Curie−Paris 6, ESPCI, 10 rue Vauquelin, F-75005 Paris, France, and SESO, CNRS UMR 6510, Université de Rennes 1, Bât.10A, 263 Av du Général Leclerc, 35042 Rennes, France

Received October 5, 2005. In Final Form: December 16, 2005

Semiconductor colloidal quantum dots (QDs) are promising fluorescent probes for biology. Initially synthesized in organic solvents, they can be dispersed in aqueous solution by noncovalent coating with amphiphilic macromolecules, which renders the particles hydrophilic and modifies their interactions with other biological compounds. Here, after coating QDs with an alkyl-modified polyacrilic acid, we investigated their colloidal properties in aqueous buffers by electrophoresis, electron microscopy, light scattering, and rate zonal centrifugation. Despite polymer dispersity and variation of the size of the inorganic nanoparticles, the polymer−dot complexes appeared relatively well-defined in terms of hydrodynamic radius and surface charge. Our data show that these complexes contain isolated QD surrounded by a polymer layer with thickness 8−10 nm. We then analyzed their interaction with giant unilamellar vesicles, either neutral or cationic, by optical microscopy. At neutral pH, we found the absence of binding of the coated particles to lipid membrane, irrespective of their lipid composition. An abrupt surface aggregation of the nanoparticles on the lipid membrane was observed in a narrow pH range (6.0−6.2), indicative of critical binding triggered by polymer properties. The overall features of QDs coated with amphiphilic polymers open the route to using these nanoparticles in vivo as optically stable probes with switchable properties.

Introduction

Semiconductor quantum dots (QDs) represent a new class of fluorescent labels with a growing number of biological and medical applications.[1−5] These emitters, also known as nanocrystals in reference to their small size (2−10 nm diameter range) and structure, possess unique optical properties due to strong quantum confinement effects and present many advantages over conventional dyes. First, their broad absorption spectra, combined with narrow and symmetric emission peaks, enable multicolor analysis with a single excitation line and without spectral cross talk between different detection channels. Second, their high quantum yield and remarkable photostability make QDs especially suitable for ultrasensitive detection of biomolecules, possibly at the single molecule level.[6] Third, semiconductor QDs can be detected in electron microscopy, possibly providing their ultrastructural localization in a biological environment.[6]

However, semiconductor quantum dot applications in biological systems have long been limited by the difficulty in obtaining water-soluble nanoparticles. As synthesized in organic solvents, QDs are coated with a hydrophobic outer shell made of surfactant trioctyl phosphine oxide (TOPO) molecules and do not disperse in aqueous buffers. To overcome this problem, QDs need to be solubilized in a manner that maintains their optical properties and permits further bioconjugation.

In past years, many strategies have been, and are still being, designed to make QDs water-soluble and biocompatible. These strategies can be separated into two different approaches: surface−ligand exchange and coating of the QDs with additional layers of molecules. In the former, the TOPO molecules are replaced with bifunctional molecules, such as cysteines,[7] mercapto alkanoic acids,[2,8] or oligomeric phosphines.[9] The resulting particles are covered by a monolayer of ligands with a hydrophilic group (carboxyl, amine, or alcoholic) facing the solution and a binding group, such as a mercapto group, attached to the ZnS surface. However, the desorption of mercapto compounds may lead to a reduced long-term colloidal stability of the nanocrystals. This limitation can be overcome when the ligand possesses multiple mercapto groups simultaneously binding to the QD, as was recently shown in the case of peptidic chains attached to QDs by six cystein residues[10] or when additional cross-linking between the capping groups is performed.[11] A slow oxidation of quantum dots can, however, happen and might cause degradation of QD optical properties.[12] In the second approach, TOPO molecules are not removed but interact with the hydrophobic part of amphiphilic molecules. The hydrophilic part, which is exposed to the solvent, ensures the solubility and enables

* Corresponding authors. E-mail: christophe.tribet@espci.fr (C.T.); maxime.dahan@lkb.ens.fr (M.D.).

[†] Ecole normale supérieure et Université Pierre et Marie Curie.

[‡] CNRS UMR 7615 et Université Pierre et Marie Curie.

[§] Université de Rennes 1.

(1) Bruchez, M., Jr.; Moronne, M.; Gin, P.; Weiss, S.; Alivisatos, A. P. *Science* **1998**, *281*, 2013−6.

(2) Chan, W. C.; Nie, S. *Science* **1998**, *281*, 2016−8.

(3) Michalet, X.; Pinaud, F.; Bentolila, L. A.; Tsay, J. M.; Doose, S.; Li, J. J.; Sundaresan, G.; Wu, A. M.; Gambhir, S. S.; Weiss, S. *Science* **2005**, *307*, 538−44.

(4) Jaiswal, J. K.; Simon, S. M. *Trends Cell Biol.* **2004**, *14*, 497−504.

(5) Medintz, I. L.; Uyeda, H. T.; Goldman, E. R.; Mattoussi, H. *Nat. Mater.* **2005**, *4*, 435−46.

(6) Dahan, M.; Levi, S.; Luccardini, C.; Rostaing, P.; Riveau, B.; Triller, A. *Science* **2003**, *302*, 442−5.

(7) Sukhanova, A.; Venteo, L.; Devy, J.; Artemyev, M.; Oleinikov, V.; Pluot, M.; Nabiev, I. *Lab. Invest.* **2002**, *82*, 1259−61.

(8) Åkerman, M. E.; Chan, P.; Laakkonen, S. N.; Bhatia, E.; Ruoslahti, E. *Proc. Natl. Acad. Sci. U.S.A.* **2002**, *99*, 12617−12621.

(9) Kim, S.; Bawendi, M. G. *J. Am. Chem. Soc.* **2003**, *125*, 14652−3.

(10) Pinaud, F.; King, D.; Moore, H. P.; Weiss, S. *J. Am. Chem. Soc.* **2004**, *126*, 6115−6123.

(11) Gerion, D.; Pinaud, F.; Williams, S. C.; Parak, W. J.; Zanchet, D.; Weiss, S.; Alivisatos, A. P. *J. Phys. Chem. B* **2001**, *105*, 8861−8871.

(12) Aldana, J.; Wang, Y. A.; Peng, X. *J. Am. Chem. Soc.* **2001**, *123*, 8844−50.

10.1021/la052704y CCC: $33.50 © xxxx American Chemical Society
Published on Web 01/26/2006 PAGE EST: 6.7

additional functionalization. This procedure has been successfully carried out with different amphiphilic molecules, leading to QDs encapsulated in phospholipid micelles[13,14] or covered by a shell of polymers.[15−18]

In light of the growing number of solubilization procedures and of biological applications of QDs,[3,5] it becomes critical to investigate not only the biochemical properties but also the colloidal properties of the solubilized nanoparticles. Depending on the solubilization method, important quantities such as the charge or the hydrodynamic radius can be expected to significantly vary and to affect the interactions of the QDs with their biological and biochemical environment. It is thus likely that the solubilization strategy should be adapted according to the biological system under study.

In this Article, we propose a simple method to produce new fluorescent markers by combining the superior brightness of CdSe/ZnS semiconductor quantum dots with the amphiphilic properties of the amphipol polymers (AP), which are commonly used to handle membrane proteins in aqueous solutions[19] and are similar to polymers used in commercial QDs.[15] Amphipols, which have a hydrophilic backbone with hydrophobic side chains, interact with the QD hydrophobic surface, forming a noncovalent but stable layer at the interface between the ZnS outer shell and the aqueous solution. The amphipol-coated QDs (APQDs) were characterized by capillary electrophoresis, quasi elastic light scattering, transmission electron microscopy, and ultracentrifugation in sucrose gradient. Altogether, our measurements showed that solubilization by the amphipols leads to monodisperse solutions of nanoparticles with features (colloidal stability, hydrodynamic radius) close to those of commercial quantum dots. As a first step to determine the practical conditions for the use of APQDs in cell biology, we studied their interaction with giant unilamellar vesicles (GUVs) used as a model of lipid membrane. The role played by the charges or charge patches on this interaction was probed using GUVs comprised of cationic or neutral lipids. We observed the importance of pH as a regulating parameter of the interaction and that in common biological buffers at neutral pH, no interactions occur between QDs and neutral or positively charged GUVs.

Materials and Methods

Synthesis of ZnS-Coated CdSe Quantum Dots. In this work, we used ZnS-coated CdSe quantum dots synthesized using standard protocols[20] and emitting at different wavelengths: 528, 534, 558, 586, and 620 nm. The samples had emission spectra with a full width at half-maximum of 30−35 nm and a quantum yield in the range 0.2−0.5. Their colloidal properties were compared, after solubilization with amphipols (APQDs), to those of commercial quantum dots (QD605 coupled to streptavidin and QD655 coupled to Goat F(ab')2 anti-Mouse IgG, Quantum Dot Corp.).

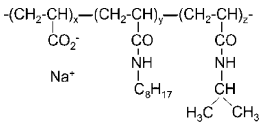

Figure 1. Structure of the amphiphilic polymer ($x = 0.35$, $y = 0.25$, $z = 0.4$, random terpolymer).

Amphipol Structure. AP were obtained by the successive reactions of octylamine and isopropylamine on a poly(acrylic acid) precursor dissolved in *N*-methyl-2-pyrrolidone, in the presence of dicyclohexylcarbodiimide as activating agent, yielding a random grafting of hydrophobe side groups.[21] The basic form of the polymer was obtained by neutralization with sodium methanoate, followed by ∼10× dilution in water. Purification was achieved by three cycles of filtration, polymer precipitation in acid aqueous media (HCl), centrifugation, and redissolution in NaOH/water. In this study, we used amphipol 5-25C8-40C3, derived from a poly(acrylic acid) parent of nominal molecular weight 5000 g/mol (Aldrich), polydispersity ∼2, and comprising 25 ± 2 mol % of C8 (octylacrylamide units) groups and 40 ± 4 mol % of C3 (isopropylacrylamide) (Figure 1).

Quantum Dot Solubilization with Amphipols. After synthesis, the CdSe/ZnS quantum dot concentration was estimated by recording the OD (optical density) and using published values for the extinction coefficient.[22] CdSe/ZnS QDs were precipitated from the initial butanol stock solution with methanol, rinsed with methanol, and dried under vacuum. QDs were then redispersed in a 10 mg/mL amphipol solution in chloroform. The molar ratio of amphipols and QDs was kept above 500:1 because using lower ratios led to the formation of large aggregates. The tube containing the mixture of AP and QDs was put in a boiling water bath. After complete evaporation of the chloroform, the residue was dissolved in water, resulting in an optically clear solution. Free amphipol micelles and possible aggregates were removed with two runs of ultracentrifugation at 150 000*g* for 30 min each (Beckman air driven ultracentrifuge, rotor A-110) in a tube in which a droplet of 15% sucrose had been added. After centrifugation, aggregates were stuck to the bottom of the tube. The amphipol-coated QDs (visible in fluorescence with a UV lamp) were in the viscous phase of the supernatant and could be easily separated from AP micelles in the fluid part. Solubilized QDs were then recovered and resuspended in water or in the appropriate buffer (with ionic strength less than 250 mM). The purified solution of APQDs could then be stored in the dark for at least 2 months without any aggregate or precipitate formation. After solubilization, we observed a relative decrease in fluorescence quantum yield by about 30%.

Agarose Gel Electrophoresis. Measurements were carried out on agarose gels prepared at 1% in 0.25% TBE migration buffer (89 mM TRIS, 89 mM borate and 2 mM EDTA, pH 8.3). After a 40 min run, fluorescent bands were detected by illuminating the gel with an UV trans-illuminator.

Capillary Electrophoresis. Experiments were performed on a Beckman PACE-MDQ system equipped with a UV−visible diode array detector. Samples were loaded in a bare silica capillary of 31 cm × 75 μm (J&W scientific), and separation was conducted at constant voltage (6 or 12 kV with phosphate or borate run buffer, respectively, see below) and temperature 25 °C. Detection was obtained in the wavelength window 195−215 nm, where both polymer and QD absorb light. The capillary was flushed daily with 0.1 M NaOH for 10 min and rinsed with water, prior to equilibration with the run buffer (0.4 wt % boric acid and 0.3 wt % sodium borate, pH = 9.3, or 50 mM NaH_2PO_4−NaOH pH = 6.8). A run was comprised of a 5 min rinse with buffer, hydrodynamic injection of a short zone of ca. 0.5 wt % mesityloxide solution in buffer (the neutral marker of electro-osmotic flow, injected for 5 s under 0.1 psi), hydrodynamic injection of a short zone of sample APQDs in the same buffer (5 s, 0.5 psi), and finally separation under constant voltage with both ends of the capillary immersed in buffer. It is of

(13) Dubertret, B.; Skourides, P.; Norris, D. J.; Noireaux, V.; Brivanlou, A. H.; Libchaber, A. *Science* **2002**, *298*, 1759−62.
(14) Geissbuehler, I.; Hovius, R.; Martinez, K. L.; Adrian, M.; Thampi, K.; Ravindranathan, T.; Vogel, H. *Angew. Chem., Int. Ed.* **2005**, *44*, 1388−1392.
(15) Wu, X.; Liu, H.; Liu, J.; Haley, K. N.; Treadway, J. A.; Larson, J. P.; Ge, N.; Peale, F.; Bruchez, M. P. *Nat. Biotechnol.* **2003**, *21*, 41−6.
(16) Pellegrino, T.; Manna, L.; Kudera, K.; Liedl, T.; Koktysh, D.; Rogach, A. L.; Keller, S.; Radler, J.; Natile, G.; Parak, W. P. *Nano Lett.* **2004**, *4*, 704−7.
(17) Gao, X.; Cui, Y.; Levenson, R. M.; Chung, L. W.; Nie, S. *Nat. Biotechnol.* **2004**, *22*, 959−60.
(18) Kim, S. W.; Kim, S.; Tracy, J. B.; Jasanoff, A.; Bawendi, M. G. *J. Am. Chem. Soc.* **2005**, *127*, 4556−4557.
(19) Popot, J. L.; Berry, E. A.; Charvolin, D.; Creuzenet, C.; Ebel, C.; Engelman, D. M.; Flötenmeyer, M.; Giusti, F.; Gohon, Y.; Hervé, P.; Hong, Q.; Lakey, J. H.; Leonard, K.; Shuman, H. A.; Timmins, P.; Warschawski, D.; Zito, F.; Zoonensa, M.; Pucci, B.; Tribet, C. *Cell. Mol. Life Sci.* **2003**, *60*, 1559−1574.
(20) Dabbousi, B. O.; Rodriguez-Viejo, J.; Mikulec, F. V.; Heine, J. R.; Mattoussi, H.; Ober, R.; Jensen, K. F.; Bawendi, M. G. *J. Phys. Chem. B* **1997**, *101*, 9463−9475.
(21) Gohon, Y.; Pavlov, G.; Timmins, P.; Tribet, C.; Popot, J. L.; Ebel, C. *Anal. Biochem.* **2004**, *334*, 318−334.
(22) Leatherdale, C. A.; Woo, W.-K.; Mikulec, F. V.; Bawendi, M. G. *J. Phys. Chem. B* **2002**, *106*, 7619−7622.

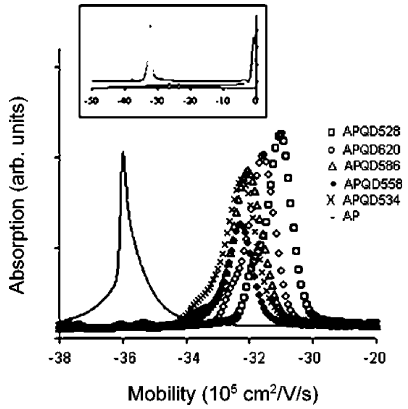

Figure 2. Capillary electrophoresis of different APQD samples and AP in 0.4 wt % boric acid and 0.3 wt % sodium borate, pH = 9.3. Inset: migration of APQD534 in 50 mM phosphate pH = 6.8.

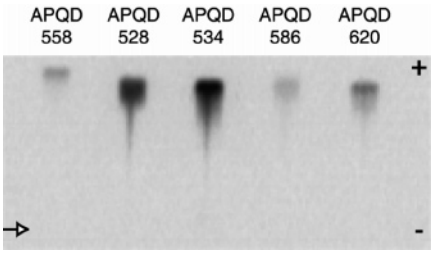

Figure 3. Amphipol-coated quantum dot separation by agarose gel electrophoresis. After purification, samples were made run on a 1% agarose gel in 0.25% TBE for 40 min at 80 V. The arrow indicates the loading position.

importance to note that the sensitivity for detection of AP in phosphate buffer was estimated in this condition to 0.2 g/L, a concentration 50-fold below the concentration used to form APQD particles.

Transmission Electron Microscopy (TEM). Transmission electron microscope images were taken on a high-resolution Philips Technai microscope at an accelerating voltage of 80 kV. Quantum dots emitting at 528 nm, in toluene solutions, were deposited on carbon copper grids covered by an amorphous carbon film 3−4 nm of thickness (Ted Pella Inc., # 01822-F). One drop of this solution at 50 nM was allowed to dry overnight. Quantum dot size distributions were determined by MetaMorph (Universal Imaging System). For QD528, the average diameter of the core−shell nanoparticles was 4.3 ± 2.2 nm (Figure 4B), in agreement with the value expected from their emission wavelength.

QELS Measurements. An ionized argon laser (SP2020, Spectra Physics, CA, 3 W) was used in QELS experiments. The laser was tuned at a wavelength of 514.5 nm. Detection optics and a photomultiplier (PCS5, Malvern Instruments, England) were mounted on a rotating arm that allowed measurements at scattering angle from 30° to 150°. All measurements were performed at a scattering angle of 90° and at 25 °C. All solutions were filtered through 0.45 μm Millipore filter directly into the cleaned scattering cell. The scattering of toluene was used as a standard intensity. APQDs samples were diluted at a final concentration of ∼300 nM in either 50 mM phosphate buffer pH = 6.8 (ionic strength 80 mM) or 50 mM boric acid−NaOH buffer pH = 9.2 (ionic strength 37 mM). For QELS, a digital correlator (K7025, Malvern Instruments, England) calculated the intensity autocorrelation function $G(q,t)$ (with q as the amplitude of the scattering vector given by $q = (4\pi n/\lambda)\sin(\theta/2)$, where n is the refractive index of the medium). Analysis of $G(t)$ in terms of a distribution of relaxation modes was achieved using REPES.[23] The corresponding diffusion coefficient D and apparent hydrodynamic radii were obtained from the mean relaxation times τ of each mode as $D = 1/\tau q^2$, and $R_h = kT/(6\pi\eta D)$ (where k is the Boltzmann constant, T is the absolute temperature, and η is the viscosity of the solvent).

Ultracentrifugation in Sucrose Gradients. Purified APQDs samples in water were diluted in 20 mM NaH_2PO_4−NaOH buffer pH = 6.8 down to a concentration of QDs ≈ 10−50 nM. Next, 100 μL of these mixtures was layered onto 4 mL of 5−20% (wt/wt) linear sucrose density gradients containing the same buffer. The tubes were centrifuged at 25 000 rpm, 25 °C, in a Beckman MLA ultracentrifuge (MLS 55 rotor, 50 200g). The positions of the fluorescent bands containing quantum dots were regularly recorded, at increasing centrifugation times typically 90, 140, and 230 min to obtain the corresponding mean sedimentation velocities with increasing penetration depth in the gradient (i.e., down to a motion through ∼$^2/_3$ of the tube length for each band considered). The absence of QD pellets in the bottom of the tube was carefully checked. Measured velocities were compared to velocities calculated as described by C. McEven[24] by integration of the instantaneous rate of sedimentation $s\omega^2 r$ (s is the sedimentation coefficient given in eq 1, r is the distance to the center of rotation, and ω is the angular velocity) along the tube, taking into account variations of viscosity and density of the sucrose gradient.

Preparation of Giant Unilamellar Vesicles. Giant unilamellar vesicles (GUVs) were obtained with the electric swelling method.[25] Two kinds of GUVs were prepared in a chloroform/methanol mixture 9:1 v/v: one made of 100% egg phosphatidylcholine (EPC) and the other made of 95% EPC and 5% 1,2-dioleoyl-3-trimethylammonium-propane (chloride salt) (DOTAP) (in molar mass). In both cases, 10 μL of a 10 mg/mL lipid stock solution was spread on each of two glass plates coated with an indium tin oxide conducting film and vacuum-dried for 45 min to obtain lipid layers. The two glass slides were assembled face-to-face by a rubber spacer to form an isolating cell, which was filled with a 50 mM phosphate buffer (5 < pH < 7 depending on the experiment) supplemented with 50 mM sucrose and 0.05% sodium azide. An electric alternating-current voltage (0.5 V, 10 Hz) was applied to this cell and increased to 1.5 V for 12 h. This method produces giant unilamellar vesicles (average diameter is 10 μm). A drop of GUVs was then transferred on a Petri dish, diluted (lipid final concentration 0.5 mg/mL) in aqueous buffer (50 mM phosphate and 50 mM glucose at various pH), and mixed with APQDs at ∼60 nM. Once sedimented GUVs were observed either by phase contrast or by epifluorescence on an inverted microscope (Olympus, IX70) equipped with a 60X objective (NA

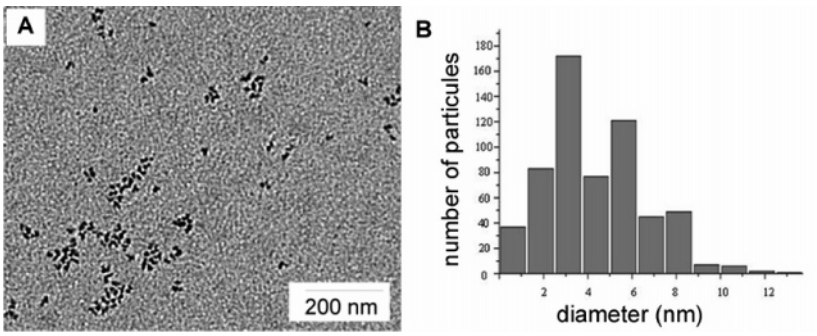

Figure 4. (A) TEM image of hydrophobic QD528 in toluene deposited on carbon copper grids. (B) Size distribution of QD528. Average diameter 4.3 ± 2.2 nm.

= 1.4, Olympus), QDs were excited at 488 nm by a UV lamp. Images were acquired by a charge coupled device (CCD) camera (CoolSnap ES, Roper Scientific).

Results

When solubilizing QDs in water, the primary goal is to obtain aqueous solubility with no loss of the monodispersity of the initially hydrophobic particles. It was achieved by a simple two-step procedure: (1) formation of a dry film from a solution of QDs and AP in chloroform, and (2) solubilization in aqueous solution followed by ultracentrifugation to remove unbound AP and possibly trace amounts of QD aggregates (see Materials and Methods). We then resorted to a variety of complementary physical methods: (i) to determine conditions under which essentially monodisperse and stable dispersions of particles are obtained, and (ii) to characterize the surface charge and the size in solution of the solubilized nanoparticles.

Using both a high AP/QD molar ratio in chloroform and a low ionic strength of aqueous solution turned out to be crucial to diminish the fraction of aggregates and achieve good monodispersity. In the following, we describe the information gathered on samples obtained by dispersing in pure water the dry film of AP and QDs prepared at a molar ratio AP/QD $\approx$ 500 and by centrifuging them prior to adding buffer.

Surface Charge and Homogeneity of APQDs. The anionic nature of AP makes it possible to investigate the homogeneity of surface coating by measurements of the electrophoretic mobility of AP-coated particles. Migrating colloids in dilute buffer solutions resolves the species in terms of their surface charge density. The results of capillary electrophoresis measurements of APQDs in borate buffer at pH = 9.3 are representative of all samples tested (Figure 2). A sharp peak is obtained at a negative mobility value, and no other species are detected in the experimental window (mobility range -66×10^{-5} to $+100 \times 10^{-5}$ cm^2/V·s) except for the co-injected reference neutral marker. Therefore, the dispersed APQDs appear well-defined in terms of surface charge density. Their mobility was remarkably constant and equal to $\sim -32 \times 10^{-5}$ cm^2/V·s (with an uncertainty of ca. 2×10^{-5} cm^2/V·s) (Figure 2). The size of the inorganic component of APQDs has therefore no effect on their migration rate, which is comparable to the one of AP (mobility of AP: -34×10^{-5} cm^2/V·s). In similar conditions, commercial dots (QD605 coupled to streptavidin and QD655 coupled to Goat F(ab')2 anti-Mouse IgG, Quantum Dot Corp.) migrated with mobility equal to $(-10 \pm 1) \times 10^{-5}$ and $(0 \pm 2) \times 10^{-5}$ cm^2/V·s, respectively, which pointed to quasi-neutral surfaces.

The charge of AP depends on pH, which may have important consequences when handling APQDs in physiological conditions. Electrophoretic analysis performed in 50 mM phosphate buffer pH = 6.8 showed that the mobility of APQDs was increased by ~10% at neutral pH, corresponding to a mobility of $-(36 \pm 1) \times 10^{-5}$ cm^2/V·s (Figure 2, inset). AP are fully ionized at pH = 9.3 and cannot have a higher charge density at pH = 6.8. The observed increasing rate of migration, if significant, may therefore reflect minor modifications of the size of APQDs. These changes could possibly result from a reduction in the self-repulsion of the amphipol side chains due to the higher ionic strength of the phosphate buffer.

Migration in agarose gels is a convenient technique to check the homogeneity of coated QDs in terms of charge/size ratio, with a good resolution in particle size over the range 3−20 nm at constant charge density. During gel electrophoresis in TBE buffer (pH = 8.3), samples migrated in a narrow predominant band, suggesting the homogeneity of the APQDs. The migration velocity of this band did not depend on the core size of the QD particles (Figure 3). When combined with the results of capillary electrophoresis, this observation suggests that all APQDs have a similar radius, irrespective of their inorganic content.

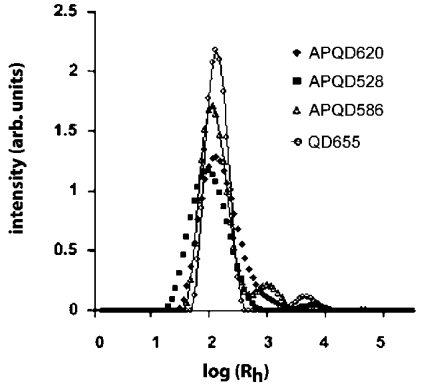

Figure 5. QELS size distributions (R_h in Å) of APQD samples in 50 mM phospshate buffer pH = 6.8 and commercial QD655.

Table 1. Intensity and Size Associated with REPES Modes in Samples of APQDs[a]

sample	R_h (nm)	I (in %)
APQD620	12	40
	47	52
APQD528	13	86
	agg	12
APQD586	14	90
	110	10
APQD534	11	70
	68	24
QD655	15	95
QD605	20	93

[a] APQDs were freshly diluted in buffer (dilution by 10× from water dispersion). Modes with a fraction of intensity below 5% are not reported.

Size and Colloidal Stability of APQDs. To estimate the hydrodynamic radius of APQDs, we performed quasi-elastic light scattering (QELS) measurements in buffer solutions. Table 1 and Figure 5 summarize the results of measurements performed at a final concentration of ~300 nM of APQDs in borate buffer. REPES distributions in size exhibit one or two modes, with a predominant mode associated with the smaller radius. Samples were also analyzed in more dilute solutions and at other scattering angles (data not shown). The absence of variation with angle by more than the uncertainty (2 nm) of the smallest apparent radius indicates the diffusive nature of the mode and the relevance of an analysis in terms of hydrodynamic radius (Figure 5). The average of the apparent hydrodynamic radii associated with each mode is given in Table 1. QELS measurements in phosphate buffer led to very similar results with no variation of the hydrodynamic radius (within the uncertainty of our measurement, ca. 1−2 nm) and of the fraction of aggregates.

The high intensity in REPES distributions of 11−13 nm-particles as compared to ca. 50−100 nm aggregates strongly suggests that small particles have an overwhelming weight fraction. Aggregates formed by a random association of particles most typically have a molecular weight MW scaling as R^α with R being the radius and α an exponent comprised between 2 and 3. In the most pessimistic case where MW $\propto R^2$, a fraction of

(23) Stepanek, P. In *Dynamic Light Scattering: the method and some applications*; Brown, W., Ed.; Clarendon Press: Oxford, U.K., 1993; Chapter 4, pp 177−241.
(24) McEwen, C. R. *Anal. Biochem.* **1967**, *20*, 114−149.
(25) Angelova, M. I.; Dimitrov, D. S. *Mol. Cryst. Liq. Cryst.* **1987**, *152*, 89−104.

intensity corresponding to aggregates of 10−20% amounts to a weight fraction below 1% (Table 1).

In general, we could obtain a fairly sharp distribution with few aggregates (e.g., APQD534, APQD528, and APQD586 in Figure 5). The stability of the size distribution was checked by incubation at room temperature in buffer and regular measurements for 2 months. Incipient aggregation was detected after 2 months, but remained negligible for shorter times (data not shown). We also noticed that samples maintained in water, at neutral pH, were more stable than those kept in phosphate or borate buffer.

In the following, we focus our analysis on the particles with radius ca. 10−15 nm, with no further trial to characterize the minor fraction of aggregates. The particle radii were all very similar within the range 11−14 nm, with a variation close to the uncertainty limit (∼2 nm) (Table 1). The size of APQDs particles could therefore be considered independent of the size of the inorganic core/shell QD and about 8−10 nm larger than the radius of TOPO-coated QD in organic solvent, as directly determined from TEM images (Figure 4) or deduced from photoluminescence spectra.

We wanted to determine whether the value of the hydrodynamic radius was due to one or to several core/shell QDs encapsulated in a polymer coat. Accurate QELS-based size determinations are, however, unreliable when investigating the properties of small (and weakly scattering) species in a sample containing also a few large (and strongly scattering) particles. The dispersity of the small particles in APDQ solutions was further studied using ultracentrifugation in sucrose gradients, an approach which is much more resolutive than light-scattering techniques to investigate mixtures of closely similar particles.

The sedimentation velocity varies in proportion to the sedimentation coefficient s, which is related by Svedberg's equation (eq 1) to the molar mass M of APQDs, their specific volume ϕ' in water, the buffer density ρ and viscosity η, and the hydrodynamic radius R_h of the particles.

$$s = M(1 - \rho\phi')/N_a 6\pi\eta R_h \quad (1)$$

Semiconductor QDs have a much higher density ($\rho_{QD} \approx 5$ g/mL) as compared to polymers ($\rho_{AP} \approx 1.15$ g/mL[21]) and, therefore, dominantly contribute to the buoyant molecular mass of APQDs particles, that is, the term $M(1 - \rho\phi')$ in eq 1. APDQs with the same R_h (12 ± 2 nm) but a varying number of QDs trapped inside the polymer coat are thus expected to display sedimentation velocities split by the mass increment of their inorganic content.

We show and analyze the results for three different samples (Figure 6). For APQD528 and QD605, sedimentation measurements led to a single band, with sedimentation coefficients 20 and 55 Sv, respectively. Because these samples have comparable R_h values, this result indicates that both correspond to monodisperse nanoparticles in regard to their molar mass. Moreover, a lower value of s for APQD 528 qualitatively agrees with the fact that its inorganic core is smaller than the core of QD605. For APQD620, a more polydisperse sample as seen by DLS (Table 1), we observed three separate bands with a predominant one with $s = 56$ Sv and two others corresponding to $s = 95$ and 125 Sv.

Using $R_h = 12$ nm, $\eta = 1$ cP, and $s = 55$ Sv in eq 1, we evaluated the buoyant molecular mass of APQD620 and QD605 to be $m = 1.24 \times 10^{-21}$ kg/nanoparticle. This result is qualitatively consistent with an estimate m_e of the buoyant molecular mass of a single red-emitting core/shell QD (assuming a total radius $r = 3.5$ nm, due to a core radius 2.5 nm and shell thickness 1 nm) surrounded by an 8.5 nm thick layer of AP. Indeed, m_e results from the sum of the buoyant mass of the inorganic component $m_{QD} = 4/3\ \pi r^3 \rho_{QD}(1 - \rho_{H_2O}/\rho_{QD}) = 0.7 \times 10^{-21}$ kg and of the polymer shell $m_{AP} = 4/3\pi(R_h^3 - r^3)\rho_{AP}(1 - \rho_{H_2O}/\rho_{AP}) \approx 0.8 \times 10^{-21}$ kg. The value of m_{AP} is very probably an overestimate because it assumes that the polymer shell does not include any water.

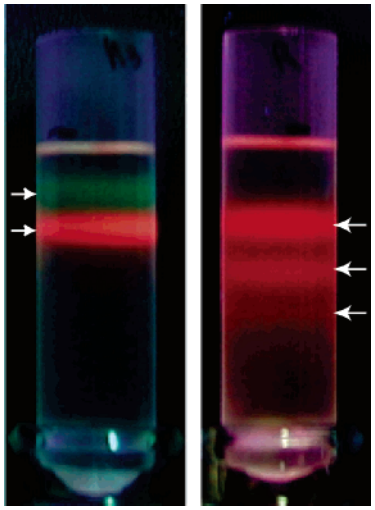

Figure 6. Rate zonal sedimentation of APQDs in 5−20% sucrose gradient. Samples were layered on the top of gradients (20 mM phosphate buffer pH = 6.8), which were centrifuged at 50 200*g* for 2 h 20 min. Left: mixtures of two samples APQD534 (upper band) and QD605 (lower band) in 20 mM phosphate buffer. Right: APQD620. Photographs are recorded under UV (365 nm) exposure.

Using the experimental value m and the calculated mass increment m_{QD} per core/shell QD (and thus a semi-experimental value for the buoyant of the polymer shell), small aggregates having the same external radius R_h, but containing two or three QDs, are expected to have buoyant masses of 1.9×10^{-21} and 2.56×10^{-21} kg, respectively. The ratio of sedimentation coefficients of oligomers to monomer is thus incremented by a step of ∼0.53 and predicted to follow the sequence 1:1.53:2.06, which is only slightly smaller than the experimental increment ∼0.6 determined in APQD620 sample (1:1.69:2.23). Note, however, that adjustment of the radius r of QD core particle by ∼10% (which is well within the experimental uncertainty) modifies this increment by ∼30%. The qualitative estimate detailed above essentially reflects the fact that the three bands observed for APQD620 are consistent with the presence of dimers and trimers in solution.

Optical Properties of APQDs. Interactions between APQDs and Giant Unilamellar Vesicles (GUVs). The use of solubilized QDs in cell biology requires that the nonspecific binding to membranes is negligible. The stability and low polydispersity of APQDs do not necessarily preclude their surface from displaying some affinity for amphiphilic lipid membranes, if, for instance, a few hydrophobic groups of the AP-coat are still accessible. We therefore probed the interactions of APQDs to lipid membranes by mixing the nanoparticles with GUVs, either neutral (EPC) or with cationic lipids (5% mol DOTAP) present in the membrane. We found that at neutral pH (phosphate buffer), APQDs do not bind to giant vesicles, irrespective of their lipid composition. Fluorescence images of GUVs mixed with APQDs at 60 nM for up to 24 h did not show any significant fluorescence of the membrane during the incubation period (Figures 7A,B and 8A,B). The shell of AP appears to develop enough repulsive forces with lipid headgroups to counterbalance the Coulombic attraction between anionic APQDs and cationic DOTAP/EPC GUVs. The spherical shape of the GUVs and the shape fluctuations were preserved over the whole incubation period. The absence of

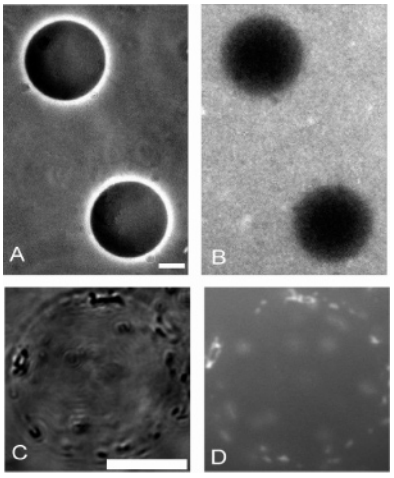

Figure 7. EPC GUVs and APQD interactions. No interactions occur between the APQDs and the EPC GUVs at neutral pH (A, transmitted light image; B, fluorescence image). Changing the pH to acidic values ($6.0 < pH < 5.0$) leads to interactions between lipids and APQDs, which arrange in clusters on the GUV surface (C and D images). Scale bar 10 μm.

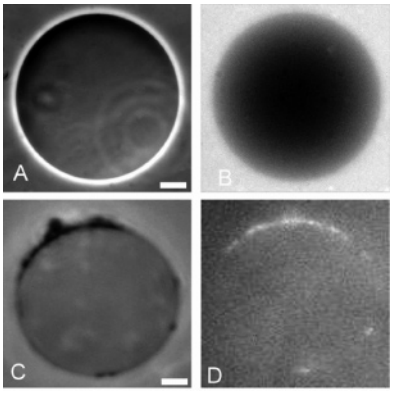

Figure 8. DOTAP GUVs and APQD interactions. At pH = 7.0, DOTAP GUVs do not interact with the APQDs (A and B images, transmitted and fluorescence light, respectively). In acidic conditions at any pH below 6.0 and down to 5.0, APQDs form clusters on the lipid membrane (C and D).

permeability to APQDs was reflected by the low internal fluorescence of GUVs having incubated during 1 day in a strongly fluorescent external bath (Figures 7B and 8B).

However, pH modulates the ionization of the AP shell, which in turn affects its hydrophilicity and its ability to repel lipid bilayers. pH-triggered interaction between AP micelles in solution and lipid bilayers can make membranes leaky or even disrupt and solubilize vesicles[26,27] with a critical pH value in the range 6.5−7.0. Neither phenomenon was observed for GUVs in the presence of APQDs and external pH in the range 5.0−9.2. Figures 7 and 8C,D show, however, that lowering the pH to 6.0 triggers within less than 5 min the binding of APQDs and the formation of highly fluorescent patches at the surface of both DOTAP/EPC and dipalmitoyl/*sn*/-glycero-3-phosphatidic acid (DPPA)/EPC. The photographs in Figures 7 and 8C,D are representative of images obtained at any pH below 6.0 and down to 5.0, with no evolution distinguishable after a 24 h-long incubation. The fluorescent patches are also detected as dark spots and large heterogeneities in phase contrast images, with no visible disruption of the membrane. In contrast, at pH above 6.2, GUVs/APQDs mixtures do not show any heterogeneity. The fluorescence in the internal compartment of GUVs remained low, suggesting the absence of penetration of APQDs through membranes, irrespective of the external pH. In addition, control images made in the pH range 5.0−6.0 but in the absence of GUVs do not show any cluster or aggregates of APQDs in solution. Therefore, aggregates of QDs form specifically at the surface of lipid membranes below a critical pH, irrespective of the membrane being neutral or cationic. The phenomenon is most likely controlled by a critical transition of a property of bound AP, reminiscent of other abrupt transitions that have been evidenced in solutions of amphiphilic polymer, such as AP-triggered vesicle disruption.[26,27]

Discussion

QELS measurement yielded hydrodynamic radii of ∼12 nm for the majority of APQDs samples, while both electrophoresis experiments and rate zonal sedimentation led to narrow migration bands. All of these results point to well-defined and homogeneous APQDs particles, in terms of both size and surface charge density. The simple solubilization method we used therefore converts hydrophobic (TOPO-capped) semiconductor QDs into hydrophilic nanoparticles and achieves excellent dispersion efficiency. This procedure was successfully applied to quantum dots of different diameters. When significant heterogeneity emerged, it was caused by aggregation and colloids instability at low pH, or after month-long incubation in buffer.

We first discuss some conclusions about the structure of the well-dispersed APQDs. Efficiency of the coating essentially refers to the TOPO molecules being masked in APQDs, which is reflected by the absence of APQDs aggregation in water. Solubilization of APQDs in water is thus certainly due to tight binding of the hydrophobic alkyl chains of the polymer on the TOPO-surfactant layer, with the outer shell of the APQDs being essentially hydrophilic. The carboxylic groups, introduced on quantum dots by the amphipol shell, add Coulombic repulsion to steric protection of the QDs. Effects of charges clearly helped in obtaining monodispersed and stable nanoparticles, with dispersions at low ionic strength providing higher stability and lower polydispersity. The stability of the sample solutions, irrespective of purification from excess AP in solution and of high dilution, strongly suggests that AP do not detach from the TOPO layer, which can be due to slow kinetics of polymer reorganization onto surfaces or to tight binding and multiple associations of C8 groups on QD surface.

The hydrodynamic radius of APDQs ranged between 11 and 14 nm (QELS), markedly larger than the radii of QDs (2−4 nm, as confirmed by TEM results). Nevertheless, rate zonal sedimentation experiments provided clear indications that a large fraction of solubilized nanoparticles consisted of a single QD encapsulated by AP. The gap in hydrodynamic radii between TOPO-coated and polymer-coated dots is thus very likely caused by a layer of AP with a thickness of 8−10 nm. Such thickness is larger than 3.6 nm, the hydrodynamic radius of AP-micelles prepared by mixing the polymer in water.[28]

In general, adsorbed monolayers of polymers are expected to have a thickness comparable to the polymer radius in solution.[29] AP similar to the ones used here adsorb on lipid membranes and form a layer thinner than ∼5 nm, while longer AP formed thicker layers.[30] Complexes of integral membrane proteins with AP also provide an interesting comparison, and a well-documented case

(26) Vial, F.; Rahbi, S.; Tribet, C. *Langmuir* **2005**, *21*, 853−862.
(27) Chen, T.; McIntosh, D.; He, Y.; Kim, J.; Tirrell, D. A.; Scherrer, P.; Fenske, D. B.; Sandhu, A. P.; Cullis, P. R. *Mol. Membr. Biol.* **2004**, *21*, 385−393.
(28) Gohon, Y.; Giusti, F.; Prata, C.; Charvolin, D.; Timmins, P.; Ebel, C.; Tribet, C.; Popot, J. L., submitted for publication.
(29) Poncet, C.; Tiberg, F.; Audebert, R. *Langmuir* **1998**, *14*, 1697−1704.
(30) Ladaviere, C.; Toustou, M.; Gulik-Krzywicki, T.; Tribet, C. *J. Colloid Interface Sci.* **2001**, *24*, 1178−187.

Scheme 1. Sketch of a Dot Complexed with Amphiphilic Polymers[a]

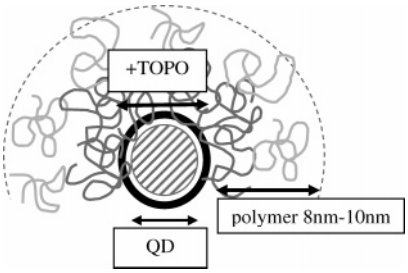

[a] QD and polymer layers are drawn to scale, with due account for all measurements of size detailed in the text.

of complexes of AP with hydrophobic particles.[19] On membrane proteins, most of the mass of AP lies in a compact layer of 1−2 nm thickness.[19] In contrast, the results on APQDs suggest that more than one polymer layer is deposited around the nanoparticule (Scheme 1). The hydrodynamic radius is, however, highly sensitive to scarce polymer chains protruding far away from the core of a particle, and the amount of AP bound on QDs might be not as extensive as depicted in Scheme 1. One could also attribute the coating thickness to a brush-like structure of the polymers on the QD surface. However, the random position of the anchoring octyl chains on the polymer makes this possibility unlikely.

Finally, the results on the interactions between APQDs and giant unilamellar vesicles demonstrate the importance of the pH as a modulating parameter of the interaction between amphipol-coated QDs and lipid membranes. The (anionic) charge density of the particle is a critical parameter for binding of polyanions onto cationic vesicles.[31,32] In common biological buffer at neutral pH, we nevertheless observed that the APQDs do not bind to EPC GUVs, or to the positively charged DOTAP/EPC. Although at pH above 6.2 a large fraction of carboxylic groups of AP are in their anionic form, it appears that the steric repulsion in the polymer layer overcomes the Coulombic attraction with DOTAP-doped membranes. This markedly differs from the negatively charged gold colloids or QD coated with 1-mercaptodecanoic acid (results to be published), which readily adsorb on DOTAP vesicles. When decreasing the pH to acidic values, APQDs become less charged, although also less hydrophilic. The rapid binding obtained at a critical pH of 6.0, together with the negligible contribution of electrostatics, point to a hydrophobic association between lipids and APQDs. The switch from almost no binding to strong clustering occurs within ∼0.2 pH units, which resembles critical transitions of polymer adsorption on solid surfaces[33] or lipid membranes.[26,27]

In regard to biological applications, our results open interesting perspectives. First, it gives physicists and biologists using APQDs as probes in cellular environment useful information on the possible nonspecific binding below a critical pH. For example, these APQDs would not be suited for imaging in acidic internal compartments such as endosomes. On the other hand, the predominant repulsion observed at pH above 6.2, even when cationic membranes were mixed with anionic APQDs, suggests that Coulombic attraction and the presence of basic proteins in membranes may not be a problem. From a practical point of view, the response to pH of polymer-coated QDs suggests new opportunities to develop sensitive sensors or triggered release of probe particles in biological media. Interestingly, critical permeabilization of endosomes has recently been observed in living cells in the presence of similar pH-responsive polymers.[34] Finally, the present study stresses the fact that using small polymer chains eliminates the difference in external size of APQDs in terms of QD core size. The large variety of grafting on the (acid groups of) polymer coat offers biochemists a tool to pair the color of particle emission with a specific surface ligand or a protein, with APQDs otherwise displaying very similar features.

Acknowledgment. We are grateful to Philippe Rostaing for his help with the TEM measurements. C.L. received a postdoctoral fellowship from CNRS. F.V. was supported by a PhD grant from Ministère de la Recherche. This work was supported by ACI DRAB (Ministère de la Recherche) and CNRS.

LA052704Y

(31) Nardi, J.; Bruinsma, R.; Sackmann, E. *Phys. Rev. E: Stat. Phys., Plasmas, Fluids, Relat. Interdiscip. Top.* **1998**, *58*, 6340−6354.
(32) Marchi-Artzner, V.; Jullien, L.; Belloni, L.; Raison, D.; Lacombe, L.; Lehn, J. M. *J. Phys. Chem.* **1996**, *100*, 13844−13856.
(33) Göbel, J. G.; Besseling, N. A. M.; Cohen Stuart, M. A.; Poncet, C. *J. Colloid Interface Sci.* **1999**, *209*, 129−135.
(34) Yessine, M. A.; Leroux, J. C. *Adv. Drug Delivery Rev.* **2004**, *56*, 999−1021.